Switching Transient Studies and Design of Neutral Grounding Reactor for Shunt-Compensated EHV Transmission Line

Md Touhidul Haque (Student ID: 1862437)
ECE 633: Modeling and Simulation of Electro-Magnetic Transients
Term: Winter 2025

Abstract— **This project presents an electromagnetic transient (EMT) simulation-based methodology for switching transient analysis and neutral grounding reactor (NGR) design in shunt-compensated extra-high voltage (EHV) transmission systems. The primary objectives are to analyze switching transient overvoltages, evaluate the effectiveness of surge arresters (SAs) and pre-insertion resistors (PIRs) as mitigation techniques, and determine an optimal NGR rating that ensures successful single-pole auto-reclosing while effectively suppressing resonant overvoltages under diverse operational scenarios. The methodology is demonstrated through a practical case study involving a 400 kV double-circuit shunt-compensated transmission line. Simulation results highlight the superior performance of PIR over SA in limiting switching transient magnitudes and damping transient oscillations. Additionally, the findings demonstrate that an optimally designed NGR can effectively balance secondary arc current suppression and resonant overvoltage control within acceptable neutral voltage limits. The study underscores the importance of evaluating both steady-state and transient performance across various operating conditions to ensure robust and reliable NGR design.**

Keywords— **Electromagnetic transient (EMT) simulation, switching transients, neutral grounding reactor (NGR), single-pole auto-reclosing, surge arrester (SA), pre-insertion resistor (PIR), secondary arc current.**

I. Introduction

Switching operations in power transmission systems, such as energization, re-energization, and fault clearance, generate transient overvoltages characterized by high-frequency oscillations and significant magnitudes. Such surges can exceed equipment insulation levels, potentially causing failures and widespread system disturbances. Therefore, comprehensive switching transient studies are crucial. They help in assessing the behavior and severity of transient voltages, quantifying overvoltage stresses, evaluating the performance of mitigation methods—such as surge arresters (SAs) and pre-insertion resistors (PIRs)—and guiding insulation coordination [1], [2].

Long extra-high-voltage (EHV) and ultra-high-voltage (UHV) transmission lines with substantial shunt compensation are particularly vulnerable to switching transients. Shunt reactors, typically compensating between 20% to 70% of the line charging capacitance, improve voltage regulation during low-load conditions [3]. However, they can introduce resonance conditions, exacerbating transient severity during switching events due to interactions between the line capacitance and reactor inductance. One common approach to manage these resonances is the use of neutral grounding reactors (NGRs) at the reactor neutral. Appropriately designed NGRs also improve arc extinction, increasing the success rate of auto-reclosing operations intended to clear single-line-to-ground (SLG) faults [4]. This enhances the overall reliability and stability of the power system. The optimal selection of NGR parameters requires comprehensive steady-state and transient studies that account for several key factors: secondary arc current and arc extinction time during single-pole auto-reclosing; induced voltages on de-energized lines during adjacent circuit energization; and resonant overvoltages during breaker failure conditions [5].

This course project proposes a simulation-based framework for analyzing switching transients and determining an optimal NGR design for a shunt-compensated EHV transmission line. The framework is demonstrated using a practical case study of a 400 kV double-circuit shunt-compensated transmission line connecting a 1600 MW thermal power plant operated by Adani in Jharkhand, India, to the 400 kV Rahanpur substation in Bangladesh. While several existing studies address switching transients and NGR design individually, the uniqueness of this work lies in its practical case-study approach and systematic validation of NGR design through detailed electromagnetic transient (EMT) simulations under diverse operating scenarios. The main contribution of this project is to conduct a realistic switching transient analysis and provide clear, detailed guidelines to help engineers and utilities design NGRs effectively for shunt-compensated EHV transmission systems.

The remainder of this report is structured as follows: Section II presents the methodology and modeling approach; Section III discusses the case study setup and simulation results; Section IV provides an in-depth discussion of the results; and Section V concludes the report with key findings and suggestions for future work. Additional technical details are provided in the Appendices.

II. Methodology

A. Switching Transient Overvoltage Study

Switching transient overvoltage studies are essential for ensuring reliable operation and proper insulation coordination of EHV and UHV transmission systems, particularly during line energization and reclosing events. This project aims to analyze transient overvoltage behavior in a shunt-compensated EHV transmission line under different switching conditions, focusing specifically on the mitigating effects of SA and PIR.

1) System Modeling: The modeling procedure for switching transient studies in this project follows established methodologies described in prior works [1], [2], [6]. The simulation model includes detailed representations of transmission lines, equivalent sources, shunt reactors, surge protection devices, and circuit breakers. Transmission lines are modeled using a frequency-dependent phase-domain model, which accurately captures high-frequency transient behavior without needing modal transformations and remains valid for untransposed lines [7]. Sending- and receiving-end substations are represented using Thévenin-equivalent sources incorporating positive- and zero-sequence impedances, since switching transients can be considered localized to the line terminals. Shunt reactors at the line terminals are modeled as linear inductances. SAs are modeled using the simplified IEEE frequency-dependent model proposed by Pinceti [8], while PIRs are represented as controlled resistive branches. Additionally, statistical variations in circuit breaker closing angles (over a 50 Hz or 60 Hz cycle) are included to capture worst-case switching transients. The models and assumptions outlined here are valid within the frequency range of interest for switching surges. Detailed descriptions of modeling procedures, assumptions, and mathematical formulations are provided in Appendix A.

2) Switching Transient Scenarios: Two primary switching scenarios are investigated to assess transient behavior:

- *Line Energization:* The transmission line is energized by closing a three-phase breaker at the sending end. This scenario examines transient overvoltages caused by line charging and traveling wave reflections.
- *Line Re-Energization:* Following initial energization and line opening, re-energization occurs after a specified dead time. This scenario assesses transient overvoltages caused by trapped charges and step potentials during rapid reclosing.

Each scenario is simulated in two modes: without any mitigation and with mitigation devices (i.e., SA or PIR) in place, to evaluate their effectiveness. In all cases, the phase-to-ground voltages at both line ends are recorded for analysis.

B. Neutral Grounding Reactor (NGR) Design

NGRs enhance the performance of shunt-compensated EHV lines by mitigating resonant overvoltages and limiting secondary arc currents during single-pole auto-reclosing events. The procedure for determining the NGR parameters follows guidelines from prior studies [3]–[5], [9], [10], which address NGR sizing for arc suppression and resonance control in compensated lines. Initially, steady-state analyses provide preliminary NGR parameters using simplified equivalent networks. Subsequently, transient studies validate these parameters by accounting for critical transient phenomena such as secondary arc current and extinction time during single-pole auto-reclosing, as well as switching overvoltages.

1) Steady-State Analysis: Steady-state analyses determine initial NGR ratings using a two-bus equivalent network model, illustrated in Fig. 1, comprising positive- and zero-sequence impedances, line impedances, admittance matrices, actual line transpositions, and shunt reactor models derived from load-flow and short-circuit analyses.

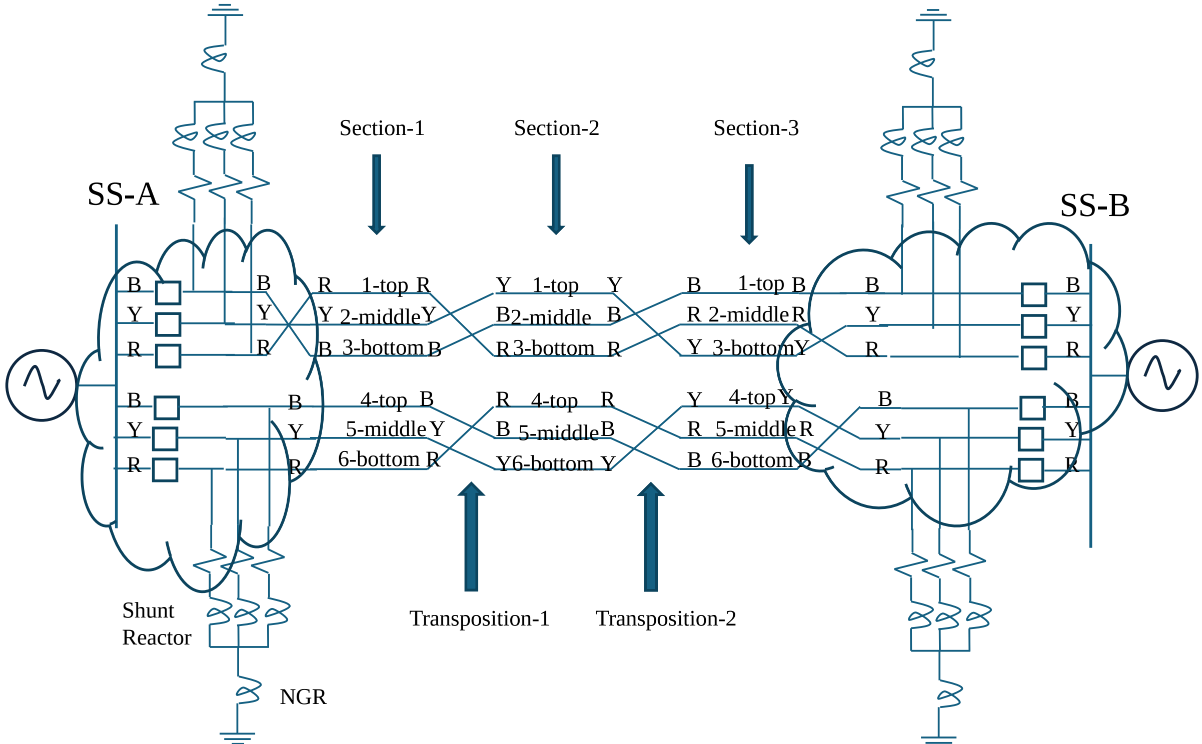

Fig. 1: Equivalent network model for NGR design study

Initially, the optimal value of the NGR to minimize steady-state secondary arc current in single-pole switching is approximated from the work of Kimbark [11]:

$$X_n = \frac{B_1 - B_0}{3FB_1\left[B_0 - (1-F)B_1\right]} \tag{1}$$

where $B_1 = \omega C_1$ and $B_0 = \omega C_0$ are the positive and zero sequence susceptances; $F = 1/(X_s B_1)$ is the shunt compensation degree; and X_s is the equivalent reactance of the line shunt reactor. The rationale behind this formula is presented in Appendix B. Based on this calculated optimal NGR value, the steady-state analysis involves the following steps:

a) Single-Pole Switching: Single-pole switching involves simulating SLG faults at strategic locations and opening the faulted phase breaker at both ends. The NGR value is varied as a percentage of the shunt reactor value. Key parameters recorded include steady-state primary and secondary arc currents, recovery voltage, rate of rise of recovery voltage (RRRV), and reactor neutral voltage and current. The selected NGR value should ensure that the steady-state secondary arc current remains below 40 A_{rms} and the RRRV below 10 kV/ms to guarantee successful secondary arc extinction [5].

b) Stuck Breaker Analysis: In this scenario, one or two circuit breaker poles are assumed to be stuck during opening, closing, or reclosing operations, resulting in open-phase conditions. When shunt compensation exceeds 65% in shunt-compensated transmission lines, these unbalanced switching conditions can cause the inductive reactance of the reactor to combine with the line capacitance, forming a resonant circuit. This resonance can generate significant temporary overvoltages, potentially damaging equipment and compromising system security [10]. The study simulates various stuck breaker cases (presented in Appendix D), varies NGR value, records open-phase voltages and reactor neutral quantities, and evaluates resonance risk.

c) Induced Voltages on De-energized Circuit: When a de-energized, shunt-compensated line runs parallel to an energized circuit (e.g., in a double-circuit configuration), high induced voltages may develop due to parallel resonance between the line's shunt reactor and its capacitance. As the NGR is connected at the shunt reactor's neutral point, it affects the damping characteristics of the ring-down voltage oscillations in the de-energized line. Therefore, its value must be carefully selected to suppress parallel resonant overvoltages.

The induced voltage study involves: (i) energizing one circuit while keeping the other de-energized, (ii) varying the de-energized circuit's NGR value, (iii) analyzing its phase-to-ground and neutral voltages, and (iv) evaluating resonance potential. The process repeats with the adjacent circuit energized and SLG faults applied at strategic locations.

In short, steady-state analyses determine the initial NGR value by meeting two criteria:

– Successful secondary arc extinction (i.e., steady-state secondary arc current < 40 A_{rms} and RRRV < 10 kV/ms)
– Suppression of resonance conditions, verified through stuck-breaker scenarios and induced voltage studies on de-energized circuits

Once these conditions are satisfied, transient analysis studies are conducted.

2) Transient Analysis: Transient studies—including single-pole auto-reclosing and line energization—validate the preliminary NGR rating. These simulations reflect dynamic behavior and practical applicability.

a) Single-Pole Auto-Reclosing: In EHV/UHV systems, single-phase auto-reclosing enhances reliability after SLG faults. The interphase capacitance and inductance sustain a secondary arc current through the opened phase's fault point, creating a recovery voltage that challenges successful reclosing. Auto-reclosure succeeds only if the secondary arc extinguishes before breaker's predefined dead time. Most EMT tools model this current using Mayr-Cassie equations [12]. An analytical description of dynamic secondary arc modeling based on Mayr and Cassie equation is presented in Appendix E. The arc extinction time t relates to the secondary arc current peak magnitude I_{sec} via [11]:

$$t = 0.25\,(0.1 \cdot I_{\text{sec}} + 1) \tag{2}$$

Single-pole auto-reclosure study is performed by applying SLG fault at strategic locations with the selected NGR value. The simulations track the secondary arc current and recovery voltage at the fault location, monitor reactor neutral quantities, and verify that the arc extinguishes before the breaker dead time expires.

b) Switching Overvoltage Study: Line energization is simulated with the selected NGR value and SA protection. Voltage peaks are measured and verified against insulation coordination limits.

A summary of NGR design process is presented in Appendix C.

III. Case Study and Results

The Adani–Rahanpur 400 kV double-circuit shunt-compensated transmission line is selected as the case study for switching transient overvoltage and NGR design. This line is a cross-border AC high-voltage corridor developed for importing power from Adani Power's Godda thermal power plant in India into the transmission grid system in Bangladesh. It spans approximately 133.7 km from the Adani 400 kV switchyard in India to the Rahanpur 400 kV substation in Bangladesh. The transmission line and system data are provided by Power Grid Bangladesh PLC, the sole transmission utility in Bangladesh, and are presented in Appendix F. System modeling and all simulations are carried out in PSCAD, a widely-used EMT simulation tool.

A. Switching Transient Results

Switching transient overvoltage study results for the Adani–Rahanpur 400 kV double-circuit transmission line are depicted in Fig. 2, and detailed circuit models and observed waveforms are provided in Appendix G. The highest peak voltage, approximately 2.76 p.u., is observed during line re-energization at the open end (Adani) without any mitigation control. While SA implementation reduces this peak to 2.08 p.u., PIR control with a 400 Ω resistor and a 10 ms delay further reduces it to 1.26 p.u., demonstrating superior performance compared to SA control.

B. NGR Design Results

1) Steady-State Analysis: Based on Eq. 1 and the system data from Appendix F, the initial NGR value is calculated as $840\,\Omega$, which is approximately 30% of the shunt reactor value.

a) Single-Pole Switching: SLG faults are applied with single-pole switching at three locations along the transmission line: Adani end, midpoint, and Rahanpur end. The NGR value is varied from 0% to 35% in 5% increments. The resulting steady-state secondary arc current, RRRV at the fault location, as well as the neutral voltage and neutral current, are presented in Fig. 3 and Fig. 4, respectively. At a 30% NGR setting, the maximum observed values are a steady-state secondary arc current of 13.5 A_{rms} and an RRRV of 5.8 kV/ms at the fault location, which remain within prescribed limits. The corresponding neutral voltage and neutral current reach 62 kV_{rms} and 45 A_{rms}, respectively.

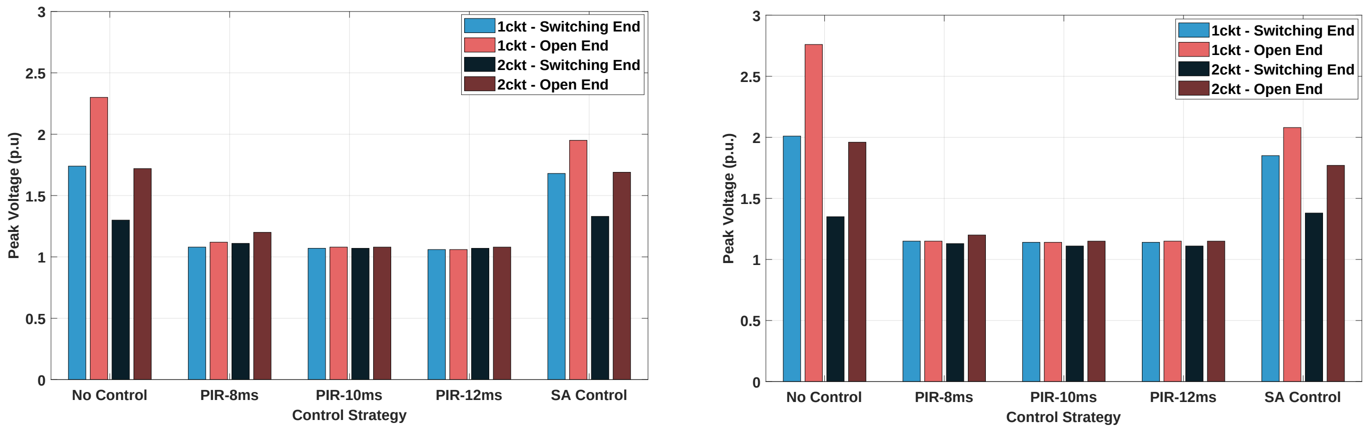

(a) Line Energization

(b) Line Re-Energization

Fig. 2: Switching transient overvoltages for line energization and re-energization with different control strategies

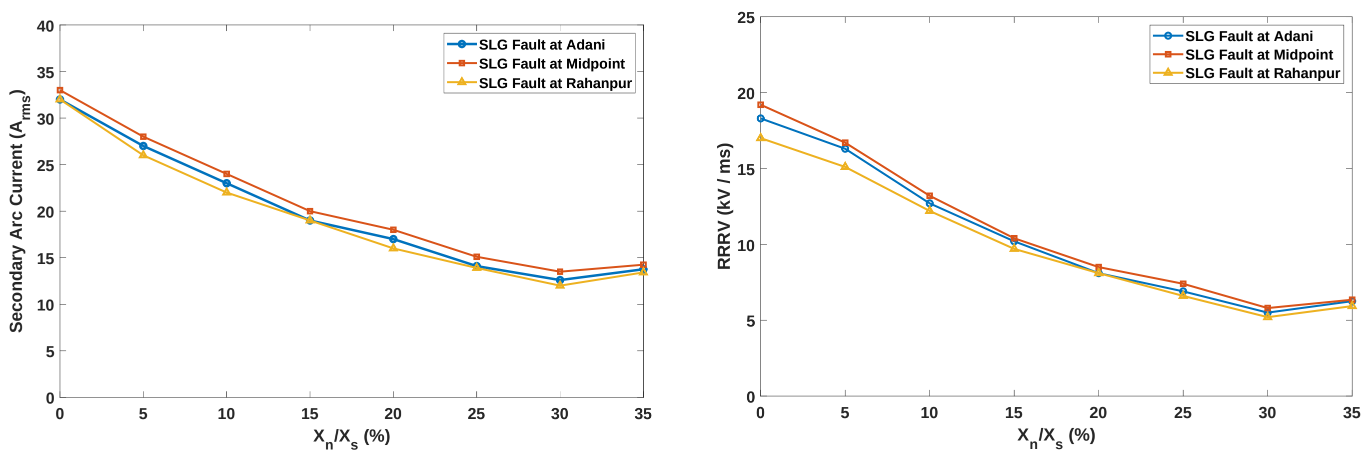

(a) Steady-state secondary arc current

(b) RRRV

Fig. 3: Steady-state secondary arc current & RRRV for SLG fault with single-pole switching as a function of NGR

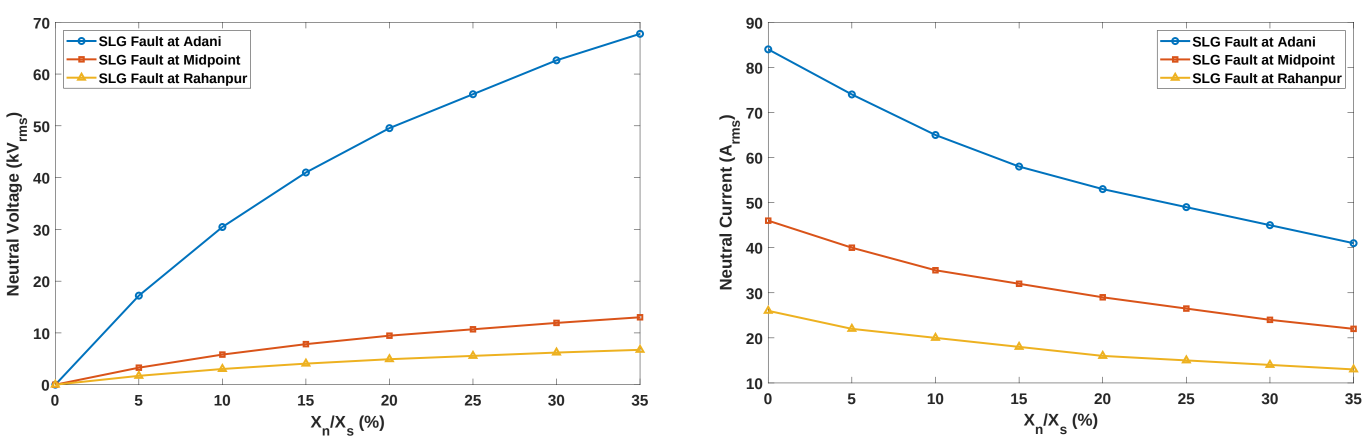

(a) Neutral voltage

(b) Neutral current

Fig. 4: Steady-state neutral voltage & current for SLG fault with single-pole switching as a function of NGR

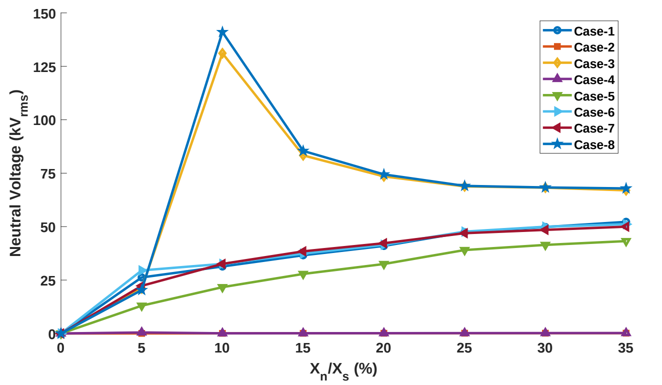

(a) Neutral voltage

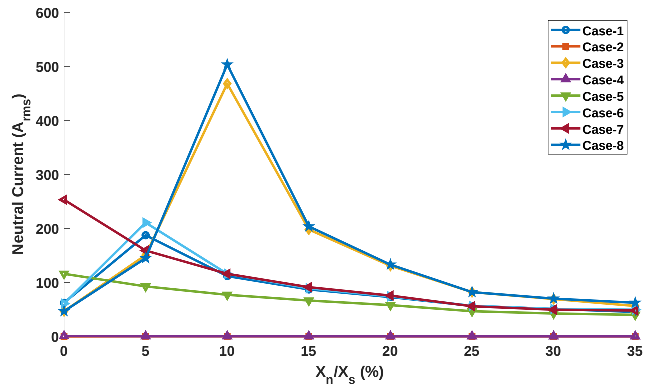

(b) Neutral current

Fig. 5: Steady-state neutral voltage and current at different stuck breaker conditions as a function of NGR

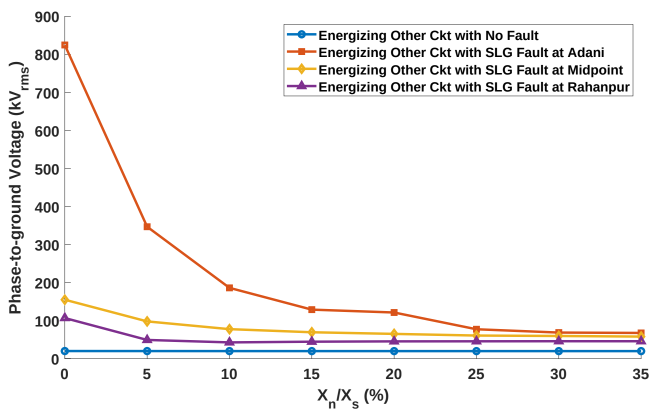

(a) Phase-to-ground voltage

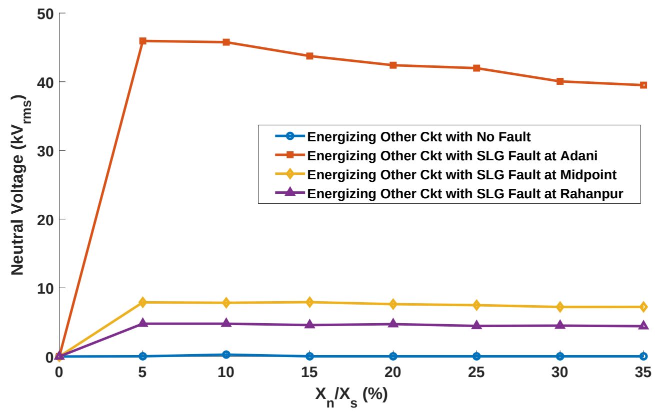

(b) Neutral voltage

Fig. 6: Induced phase-to-ground and neutral voltage on de-energized circuit during energization of the adjacent circuit with/without SLG fault

b) Stuck Breaker Analysis: Eight stuck breaker conditions (presented in Appendix D) are simulated for the Adani–Rahanpur transmission line. For each stuck breaker condition, the NGR value is varied from 0% to 35% in 5% increments. The observed steady-state neutral voltages and currents for different conditions and NGR values are shown in Fig. 5. The maximum neutral voltage and current—141 kV$_{\text{rms}}$ and 503 A$_{\text{rms}}$, respectively—are found for case-8 at 10% NGR value. For the initially selected NGR value (30% X_n/X_s), the maximum neutral voltage and current are 68 kV$_{\text{rms}}$ and 70 A$_{\text{rms}}$, which are significantly lower than those recorded at other NGR settings, demonstrating its effectiveness in mitigating resonance effects caused by stuck breaker cases.

c) Induced Voltages on De-energized Circuit: An induced voltage study is performed on the de-energized circuit for two cases: energizing the adjacent circuit, and energizing it while applying an SLG fault. For both cases, the NGR value is varied from 0% to 35% in 5% increments. The observed induced phase-to-ground and neutral voltages on the de-energized circuit are shown in Fig. 6. The highest induced phase-to-ground voltage is observed as 824 kV$_{\text{rms}}$ (approximately 3.4 p.u.) at 0% NGR value, whereas the highest neutral voltage is observed as 46 kV$_{\text{rms}}$ at 5% NGR value. At 30% NGR value, the highest induced phase-to-ground voltage and neutral voltage are found to be 68 kV$_{\text{rms}}$ and 40 kV$_{\text{rms}}$, respectively. These findings indicate that in the absence of an NGR, dangerous parallel resonance overvoltages can occur in the de-energized circuit.

2) Transient Analysis:

a) Single-Pole Auto-Reclosing: A single-pole auto-reclosure study is performed by applying SLG faults at the Adani end, midpoint, and Rahanpur end of the line, using the selected NGR value. The observed peak recovery

TABLE I: Findings of single-pole auto-reclosing study with the selected NGR of 840 Ω

SLG Fault Location	**Adani End**			**Mid-Point**			**Rahanpur End**		
Parameters Observed	Recovery Voltage (kV peak)	Secondary Arc Current (A peak)	Arc Extinction Time (s)	Recovery Voltage (kV peak)	Secondary Arc Current (A peak)	Arc Extinction Time (s)	Recovery Voltage (kV peak)	Secondary Arc Current (A peak)	Arc Extinction Time (s)
	201.38	24.74	0.87	203.87	24.75	0.87	205.11	24.73	0.87

voltages, peak secondary arc currents, and arc extinction times are presented in Table I. The maximum secondary arc extinction time is 0.87 s, which is within the 1 s dead time specified by the Grid Code of Bangladesh.

b) Switching Overvoltage Study: Line energization is performed with the selected NGR value in the presence of SA protection. The open-end (Adani side) peak phase-to-ground voltages for circuit-1 and circuit-2 are approximately 1.69 p.u. (552 kV) and 1.95 p.u. (637 kV), respectively. These values are well below the basic switching impulse level (BSIL) of 1050 kV for a 400 kV system, as per IEEE Std C62.82.1-2010 [6].

Detailed circuit models and observed waveforms from the steady-state and transient analyses for the NGR design are presented in Appendix H.

3) Recommended NGR Parameters: Based on the steady-state and transient analyses, the selected NGR value of 840 Ω (i.e., 30% of the shunt reactor value) satisfies the requirement of a steady-state secondary arc current (i.e., $<$ 40 A_{rms}), arc extinction time (i.e., $<$ breaker dead time of 1 s), and suppressing temporary resonant overvoltages. The maximum observed temporary overvoltage and current at neutral are 70 A_{rms} and 68 kV_{rms}, respectively. The complete recommended NGR parameters for the Adani–Rahanpur transmission line are given in Appendix I.

IV. Discussion

The switching transient analysis demonstrates that PIR control significantly outperforms SA control in suppressing switching overvoltages and damping oscillations in shunt-compensated EHV transmission systems. In the base case without mitigation measures, the peak phase-to-ground voltage reaches 2.76 p.u., highlighting the severity of switching transients in such systems. While SA implementation reduces this peak voltage to 2.08 p.u., representing a 24.6% improvement, PIR control with a 10 ms delay demonstrates superior performance by further reducing the overvoltage to just 1.26 p.u. – a 54.3% reduction compared to the base case and 39.4% improvement over SA performance. The superior performance of the PIR stems from its ability to dissipate energy and damp the transient from the very onset of the switching event, in contrast to the SA which only conducts above a high threshold voltage. Essentially, the PIR's temporary insertion of resistance curtails the initial surge and provides additional damping to oscillatory modes. The combined effect of peak voltage reduction and oscillation attenuation makes PIR an optimal strategy for managing switching transients in long, shunt-compensated EHV transmission lines.

The NGR design is validated through steady-state and transient simulations. Results from the single-pole switching with SLG fault case study indicate that increasing the NGR value leads to a reduction in steady-state secondary arc current, which reaches a minimum around the 30% NGR setting (i.e., 840 Ω) for the Adani–Rahanpur transmission line. Meanwhile, the neutral voltage rises with higher NGR values, indicating that increases beyond 30% yield diminishing returns in arc suppression while necessitating higher voltage ratings for the NGR. This supports the selection of 30% NGR as an optimal design point for the Adani–Rahanpur transmission line. Additionally, the arc extinction time from single-pole auto-reclosing study remains approximately 0.87 s across all fault locations, indicating that arc quenching performance is largely insensitive to fault position under the selected NGR setting. In the induced voltage study, energizing one circuit while the adjacent circuit remains de-energized and no NGR is applied results in dangerously high induced voltages—reaching 824 kV_{rms} (approximately 3.4 p.u.)—which exceeds the temporary overvoltage withstand capability of 400 kV-class switchgear. This overvoltage is attributed to parallel resonance between the line's shunt capacitance and the reactor inductance, emphasizing the role of the NGR in suppressing such conditions beyond its primary function in arc current mitigation. Furthermore, analysis of stuck breaker scenarios and induced voltages at low NGR values (e.g., 5%) reveals that specific combinations of operating conditions—particularly Case-3 and Case-8 of stuck breaker conditions—can result in significantly elevated resonant overvoltages. These findings highlight the importance of accounting for breaker failure modes and resonance phenomena when selecting NGR parameters, in order to prevent severe temporary overvoltages and protect system equipment.

V. Conclusion and Suggestions for Further Studies

This study presents a comprehensive methodology for switching transient overvoltage analysis and NGR design for shunt-compensated EHV transmission lines. The methodology is demonstrated through a detailed case study involving a real-world 400 kV double-circuit shunt-compensated transmission line.

Generalized findings from the case study highlight that PIR control offers significant advantages over SA control in mitigating switching transient overvoltages. PIR not only reduces the peak overvoltage during line energization and re-energization but also provides superior damping of high-frequency oscillations, thereby improving insulation coordination and equipment protection.

The selection of an appropriate NGR value is critical in shunt-compensated transmission systems, as it directly influences multiple performance objectives—including suppression of secondary arc currents during single-pole auto-reclosing, control of neutral voltage rise, mitigation of resonant overvoltages, and compliance with insulation coordination limits. These objectives often involve trade-offs that cannot be resolved analytically in isolation. The proposed simulation framework addresses this by evaluating both steady-state and transient performance under diverse operating scenarios such as single-pole auto-reclosing, stuck breaker scenarios, and induced overvoltage conditions. By examining all these conditions, the methodology ensures the chosen NGR provides balanced performance across competing criteria. In the case study, this leads to the recommendation of a 30% NGR, which is shown to meet arc extinction requirements and prevent excessive resonant overvoltages.

To further strengthen and generalize the proposed NGR design methodology, several directions for future research are identified. First, investigating the impact of varying system conditions—such as changes in system strength in terms of short-circuit level, variations in shunt reactor configuration using switched or variable reactor banks, changes in ground resistance—on NGR performance would help assess the robustness of the proposed NGR design across a broader range of operating scenarios. Second, further validation of the NGR selection through temporary overvoltage studies, such as load rejection and load rejection accompanied by SLG faults, is recommended to confirm compliance with equipment withstand capabilities.

Future work may also explore advanced switching transient mitigation strategies, such as coordinated PIR and controlled switching device (CSD) schemes, or the use of power electronic-based dynamic overvoltage suppressors. Additionally, incorporating nonlinear phenomena such as corona effects could enhance the accuracy and extend the range of validity of switching transient modeling, particularly for UHV transmission systems where air ionization plays a more prominent role.

References

[1] M. Cervantes, I. Kocar, A. Montenegro, D. Goldsworthy, T. Tobin, J. Mahseredjian, R. Ramos, J. Marti, T. Noda, A. Ametani *et al.*, "Simulation of switching overvoltages and validation with field tests," *IEEE Transactions on Power Delivery*, vol. 33, no. 6, pp. 2884–2893, 2018.

[2] J. A. Martinez, D. Goldsworthy, and R. Horton, "Switching overvoltage measurements and simulations—part i: Field test overvoltage measurements," *IEEE Transactions on Power Delivery*, vol. 29, no. 6, pp. 2502–2509, 2014.

[3] S. Atmuri, R. Thallam, D. Gerlach, T. Lundquist, and D. Selin, "Neutral reactors on shunt compensated ehv lines," in *Proceedings of IEEE/PES Transmission and Distribution Conference*, 1994, pp. 121–128.

[4] M. R. Dadash Zadeh, M. Sanaye-Pasand, and A. Kadivar, "Investigation of neutral reactor performance in reducing secondary arc current," *IEEE Transactions on Power Delivery*, vol. 23, no. 4, pp. 2472–2479, 2008.

[5] K. Meera and P. Bhurat, "Neutral grounding reactors for shunt compensated ehv transmission lines," in *2016 IEEE Region 10 Conference (TENCON)*, 2016, pp. 1489–1494.

[6] "Ieee guide for the application of insulation coordination," *IEEE Std C62.82.2-2022*, pp. 1–83, 2023.

[7] T. Noda, N. Nagaoka, and A. Ametani, "Phase domain modeling of frequency-dependent transmission lines by means of an arma model," *IEEE Transactions on Power Delivery*, vol. 11, no. 1, pp. 401–411, 1996.

[8] P. Pinceti and M. Giannettoni, "A simplified model for zinc oxide surge arresters," *IEEE Transactions on Power Delivery*, vol. 14, no. 2, pp. 393–398, 1999.

[9] W. Shi, F. Li, Y. Han, and Y. Li, "The effect of ground resistance on secondary arc current on an ehv transmission line," *IEEE Transactions on Power Delivery*, vol. 20, no. 2, pp. 1502–1506, 2005.

[10] V. Bathini, R. Nagaraja, and K. Parthasarathy, "Guidelines for selection of neutral reactors rating for shunt compensated ehv transmission lines," *International Journal of Engineering Research and Technology, NPSC*, 2012.

[11] E. W. Kimbark, "Suppression of ground-fault arcs on single-pole-switched ehv lines by shunt reactors," *IEEE Transactions on Power Apparatus and Systems*, vol. 83, no. 3, pp. 285–290, 1964.

[12] P. H. Schavemaker and L. Van der Slui, "An improved mayr-type arc model based on current-zero measurements [circuit breakers]," *IEEE Transactions on Power delivery*, vol. 15, no. 2, pp. 580–584, 2000.

[13] "Ieee standard for requirements, terminology, and test procedures for neutral grounding devices," *IEEE Std C57.32-2015 (Revision of IEEE Std 32-1972)*, pp. 1–83, 2016.

Appendix A
Detailed System Modeling Procedure

This appendix outlines the detailed modeling methodology used for the switching transient overvoltage study of the EHV transmission line. The adopted models are based on rigorously validated approaches from literature [1], [2], [6] and are compatible with EMTP-type simulation environments.

a) Transmission Line Modeling (Frequency-Dependent Phase-Domain Model): The transmission line is modeled using the frequency-dependent phase-domain model proposed by Noda et al. [7]. This approach avoids the use of modal transformations by directly representing frequency-dependent impedance and admittance matrices in the phase domain. The telegrapher's equations in the frequency domain are expressed as:

$$\frac{dV(x,\omega)}{dx} = -Z(\omega)I(x,\omega) \tag{3}$$

$$\frac{dI(x,\omega)}{dx} = -Y(\omega)V(x,\omega) \tag{4}$$

where $Z(\omega)$ and $Y(\omega)$ are frequency-dependent per-unit-length impedance and admittance matrices. Instead of recursive convolution in the time domain, the phase-domain response is approximated by an ARMA (Auto-Regressive Moving Average) model:

$$y(n) = \sum_{k=0}^{N} a_k x(n-k) - \sum_{k=1}^{N} b_k y(n-k) \tag{5}$$

This modeling method captures the full spectrum of switching surges and remains valid up to several MHz. It is especially effective for untransposed lines and mitigates numerical instabilities arising from mode crossing.

b) Surge Arrester (SA) Modeling (Simplified Pinceti Model): SAs are modeled using the simplified version of the IEEE frequency-dependent model as proposed by Pinceti [8]. The model as shown in Fig. A.1 consists of two nonlinear resistors (A0 and A1) with a series inductor L_0 and L_1, and an optional parallel resistor R for numerical stability:

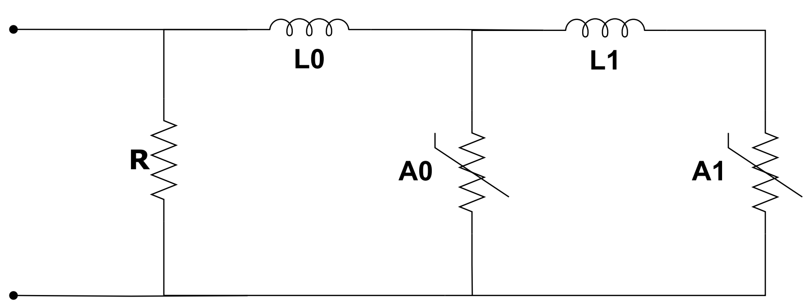

Fig. A.1: Frequency dependent surge arrester (SA) model proposed by Pinceti

- *Nonlinear Resistors (A0, A1):* Defined via standardized V-I curves referenced to $V_{r8/20}$ (residual voltage at 10 kA lightning impulse).
- *Inductances (L0, L1):* Calculated as:

$$L_1 = \frac{1}{4} \cdot \frac{V_{r1/T2} - V_{r8/20}}{V_{r8/20}} \tag{6}$$

$$L_0 = \frac{1}{12} \cdot \frac{V_{r1/T2} - V_{r8/20}}{V_{r8/20}} \tag{7}$$

where V_n = rated voltage, $V_{r1/T2}$ = residual voltage for fast-front surges (e.g., 1/5 μs).

Parameters are directly derived from standard datasheet values, avoiding iterative tuning. The model is validated for discharge currents from 1 kA to 20 kA and crest times ranging from $0.5\ \mu s$ to $45\ \mu s$.

c) Equivalent Source Modeling: The sending-end and receiving-end substations are modeled using Thévenin equivalents incorporating positive- and zero-sequence impedance:

$$Z_1 = R_1 + jX_1, \quad Z_0 = R_0 + jX_0 \tag{8}$$

Switching transients are local phenomena, and thus detailed modeling of remote system components is not necessary. The Thévenin equivalents reflect the local system strength and are sufficient for accurately replicating transient behavior over the duration of interest.

d) Shunt Reactor Modeling: Shunt reactors connected at the line ends are represented using a linear inductive model:

$$Z_{\text{reactor}} = R_r + j\omega L_r \tag{9}$$

Typical values are derived from manufacturer data or field commissioning reports.

e) Pre-Insertion Resistor (PIR) Modeling: PIRs are modeled as resistive branches that remain in the circuit for a short pre-defined duration post closing:

$$R_{\text{PIR}}(t) = \begin{cases} R_0, & 0 < t < T_{\text{PIR}} \\ 0, & t \geq T_{\text{PIR}} \end{cases} \tag{10}$$

Where R_0 is typically 400–600 Ω and T_{PIR} is 8–12 ms. Ideal switch control is used to simulate PIR bypassing after the delay.

f) Circuit Breaker Statistical Model: To replicate realistic switching conditions, the breaker poles are modeled with statistical closing angles uniformly distributed over a 50 Hz or 60 Hz cycle:

$$\theta \sim \mathcal{U}(0^\circ, 360^\circ) \tag{11}$$

This enables identification of worst-case overvoltage scenarios and supports probabilistic evaluation of switching transients.

Appendix B
Analytical Basis for the Formula of Optimal NGR Value Calculation

When a SLG fault occurs, the opened faulted phase experiences capacitive coupling from the two healthy phases. This capacitive coupling sustains a secondary arc current and generates a recovery voltage, complicating successful single-pole reclosing. Effective arc suppression thus requires neutralization of the capacitive fault current and reduction of recovery voltage across the opened phase.

Kimbark [11] analyzed this condition for uniformly transposed EHV lines by decomposing the system voltages and currents into symmetrical components: zero-, positive-, and negative-sequence modes. Consider an SLG fault on phase-a; the arc voltage across the faulted phase can be expressed in terms of symmetrical component voltages as:

$$V_a = V_0 + V_1 + V_2 \tag{12}$$

For successful arc extinction, the driving voltage across the faulted phase (arc voltage) must vanish:

$$V_a = 0 \quad \Rightarrow \quad V_0 + V_1 + V_2 = 0 \tag{13}$$

The corresponding sequence currents into the faulted node (phase-a) can be modeled in terms of their sequence admittances. According to Kimbark's analysis, these currents are:

$$I_0 = \left(B_0 + \frac{1}{3X_n}\right) V_0 \tag{14}$$

$$I_1 = B_1(1 - F)V_1 \tag{15}$$

$$I_2 = B_1 V_2 \tag{16}$$

Here, $B_0 = \omega C_0$ and $B_1 = \omega C_1$ represent the zero- and positive-sequence capacitive susceptances of the line respectively, and X_n is the NGR reactance. The parameter F is the degree of shunt compensation, defined as:

$$F = \frac{1}{X_s B_1} \tag{17}$$

where X_s is the inductive reactance per phase of the shunt reactors.

Applying Kirchhoff's Current Law (KCL) at the fault node yields the sum of sequence currents as zero:

$$I_0 + I_1 + I_2 = 0 \tag{18}$$

Substituting the expressions for I_0, I_1, and I_2 into this KCL condition, we obtain:

$$\left(B_0 + \frac{1}{3X_n}\right) V_0 + B_1(1-F)V_1 + B_1 V_2 = 0 \tag{19}$$

Utilizing the arc extinction condition $V_2 = -(V_0 + V_1)$, the above equation simplifies to:

$$\left(B_0 - B_1 + \frac{1}{3X_n}\right) V_0 - B_1 F V_1 = 0 \tag{20}$$

For non-trivial solutions (meaning non-zero voltages that represent practical conditions for arc extinction), each term in the equation should independently satisfy resonance conditions. Thus, the NGR reactance (X_n) must satisfy the resonance condition:

$$B_0 - B_1 + \frac{1}{3X_n} = 0 \tag{21}$$

Rearranging terms to isolate X_n, we get:

$$X_n = \frac{1}{3(B_1 - B_0)} \tag{22}$$

However, considering the practical effect of shunt reactors and compensation degree (F), Kimbark introduced additional relationships from the complete modal analysis. By integrating these relationships thoroughly, the complete optimal formula, which includes compensation degree explicitly, emerges as:

$$X_n = \frac{B_1 - B_0}{3FB_1\left[B_0 - (1-F)B_1\right]} \tag{23}$$

This formula is exactly the form adopted in the present report and is extensively used in industry practice. It clearly indicates the NGR value needed to minimize secondary arc currents effectively, thus enhancing the probability of successful single-pole auto-reclosing on shunt-compensated EHV transmission lines.

This derivation is based on several assumptions:

- The line is uniformly transposed and lossless.
- Capacitive coupling sustains the secondary arc without external driving voltage sources.
- Reactive components (shunt reactors and line capacitances) primarily determine the arc suppression condition.

Despite the ideal assumptions, Kimbark's analytical expression provides a reliable initial NGR value for engineering practice, which is further validated through EMT simulations under diverse operational scenarios in this study.

Appendix C
Summary of NGR Design Process

Summary of the NGR design process is presented in Table C.1.

TABLE C.1: Summary of NGR parameter selection guidelines

Parameter	Selection Criteria
Rated impedance	Based on steady-state analysis (single-pole switching, stuck breaker, induced voltage studies). Select NGR value (X_n) as a percentage of line shunt reactor (X_s) considering $\pm 2.5\%$ manufacturing tolerance.
short-time (10 sec) or thermal rated current and voltage	Derived from steady-state analysis maximum neutral current and voltage.
Continuous rated current and voltage	Calculated as 3% of short-time (10-sec) rating (IEEE Std C57.32-2015 [13]).
Rated peak current	Select the higher value between maximum initial asymmetric peak current from transient study and IEEE Std C57.32-2015 [13] computation.
Insulation level at neutral point	Based on maximum neutral voltage observed in steady-state and transient studies.
Surge arrester (SA) rating	Duty cycle of SA is selected based on short-time (10-sec) voltage rating of the NGR.

Appendix D
Various Stuck Breaker Conditions

High overvoltages may occur on de-energized circuits of shunt compensated transmission lines due to resonance triggered by stuck breaker conditions during line energization or de-energization. EHV and UHV breakers typically operate with single-pole mechanisms, but mechanical defects can result in one or more poles failing to open or close properly. This can leave one or two phases open while others are energized, creating an unbalanced condition. Shunt reactors increase open-phase voltage due to unequal compensation of positive and zero-sequence line capacitances. When compensation exceeds approximately 65%, the combination of line capacitance to ground and interphase capacitance can form a series resonant circuit with the shunt reactor. This resonance can lead to dangerously high voltages that may damage connected equipment.

The following cases are analyzed to study the impact of various stuck breaker conditions in NGR design study, as illustrated in Fig. D.1.

- Case 1: Single pole stuck breaker condition with remote end fully open and parallel line de-energized.
- Case 2: Single pole stuck breaker condition with remote end fully closed and parallel line de-energized.
- Case 3: Two pole stuck breaker condition with remote end fully open and parallel line de-energized.
- Case 4: Two pole stuck breaker condition with remote end fully closed and parallel line de-energized.
- Case 5: Single pole stuck breaker condition on either end of the line and parallel line energized.
- Case 6: Single pole stuck breaker condition on either end of the line and parallel line de-energized.
- Case 7: Two pole stuck breaker condition on either end of the line and parallel line energized.
- Case 8: Two pole stuck breaker condition on either end of the line and parallel line de-energized.

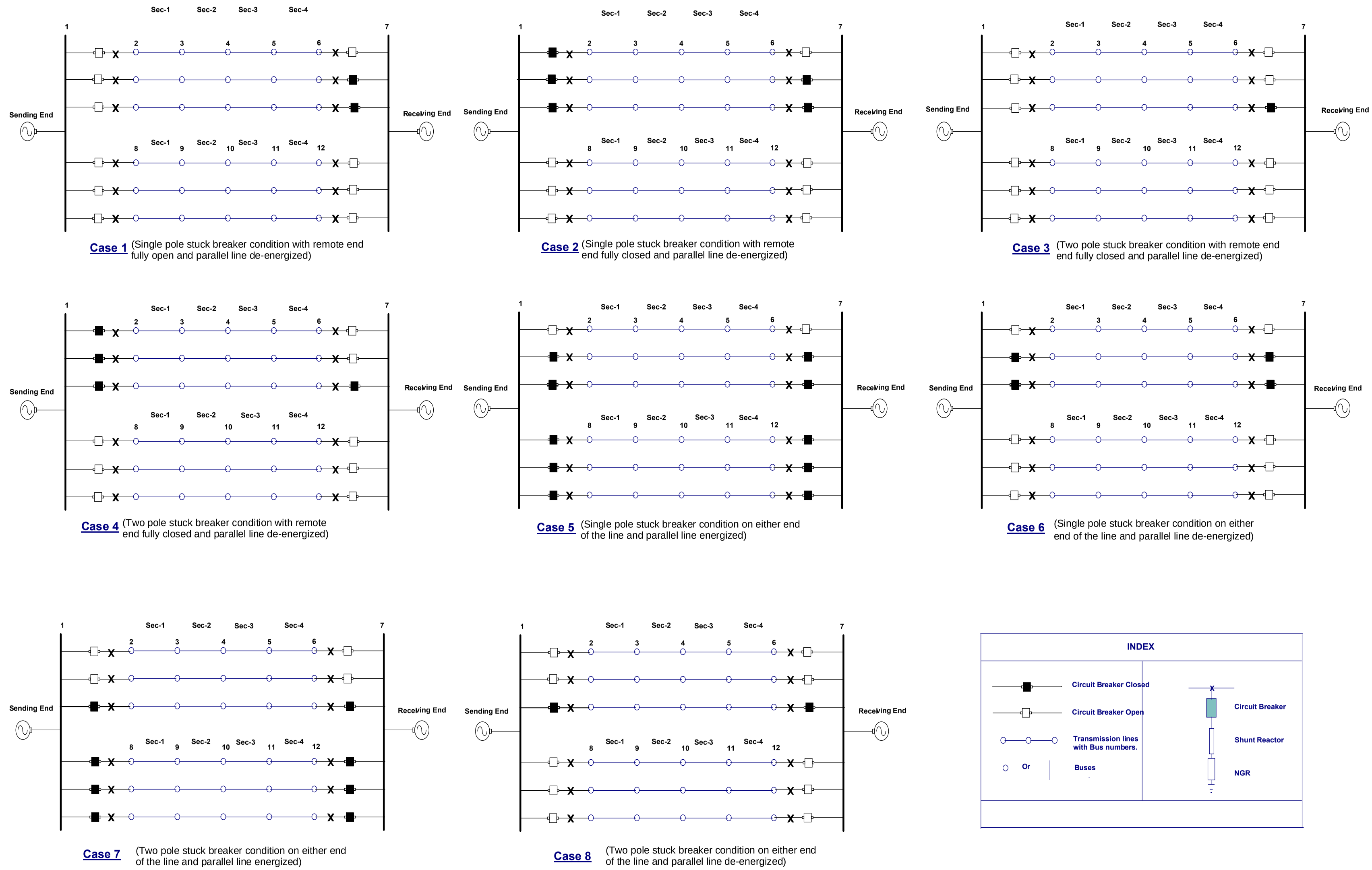

Fig. D.1: Various Stuck Breaker Conditions considered in NGR design study

Appendix E
Analytical Description of Secondary Arc Modeling Based on Mayr and Cassie Equation

Most of the EMTP-type simulation software model the secondary arc current occurring during single-pole reclosing using an improved Mayr-type arc model, originally proposed in [12]. This model offers accurate dynamic characterization of the arc near current-zero, where thermal effects dominate arc behavior.

The original Mayr arc model is formulated as a first-order nonlinear differential equation describing the time evolution of arc conductance $g(t)$:

$$\frac{1}{g}\frac{dg}{dt} = \frac{1}{\tau}\left(\frac{ui}{P} - 1\right) \tag{24}$$

where:

- g: arc conductance,
- u: arc voltage,
- i: arc current,
- τ: arc time constant (typically in the range of microseconds),
- P: arc cooling power (represents energy dissipation by the arc).

In this model, arc evolution is governed by the balance between the electrical power input ui and the cooling power P. Near current-zero, this energy balance is critical in determining whether the arc extinguishes or reignites.

To improve correspondence with measured data, Schavemaker and van der Sluis proposed a variant where the cooling power P is expressed as a function of the electrical power input:

$$P = P_0 + P_1 ui \tag{25}$$

where P_0 and P_1 are empirical cooling constants related to the breaker's physical design and plasma dynamics. Substituting (25) into (24) yields the improved arc model:

$$\frac{1}{g}\frac{dg}{dt} = \frac{1}{\tau}\left(\frac{ui}{P_0 + P_1 ui} - 1\right) \tag{26}$$

This model exhibits the following behavior:

- In the high-current region, it asymptotically approaches the Cassie model:

  $$\frac{1}{g}\frac{dg}{dt} \approx \frac{1}{\tau}\left(\frac{u}{U_{\text{arc}}} - 1\right)$$

  where U_{arc} is an equivalent constant arc voltage.
- Near current-zero, the model reduces to the classical Mayr form:

  $$\frac{1}{g}\frac{dg}{dt} = \frac{1}{\tau}\left(\frac{ui}{P_0} - 1\right)$$

  capturing the thermal instability of the arc.

The parameters τ, P_0, and P_1 are identified from high-speed current-zero measurements using least squares fitting. For the test cases analyzed in [12], typical values are $\tau = 0.27\ \mu s$, $P_0 = 15917$ W, and $P_1 = 0.9943$. These yield close agreement between simulated and measured arc waveforms.

This improved Mayr-type model is particularly well-suited for simulating secondary arc behavior in single-pole switching applications. It enables the study of arc extinction dynamics by capturing the interplay between power dissipation and conductance evolution near current zero. As such, it is used in this work to evaluate the effectiveness of NGR design in suppressing secondary arc current and facilitating successful single-pole auto-reclosing.

APPENDIX F
SYSTEM DATA FOR CASE STUDY

The system data used in the case study—including the Adani–Rahanpur 400 kV double-circuit transmission line parameters, equivalent source impedance at both substations (calculated from the fault level), and SA specifications—are provided in Table F.1, Table F.2, and Table F.3, respectively.

TABLE F.1: Adani–Rahanpur 400kV Double Circuit Line Data

Parameter	Value / Description
Transmission Line Name	Adani–Rahanpur 400 kV Double Circuit
Line Length	133.7 km
Voltage Level	400 kV
Conductor Type	Quad ACCC Dhaka
Sub-conductors per Phase	4 (Quad bundle)
Conductor Diameter	16.435 mm
Conductor DC Resistance	0.0387 Ω/km
Bundle Spacing	457.2 mm
Ground Wire Type	ACSR Dorking
Ground Wire Diameter	8 mm
Tower Configuration	Double-circuit, phase conductor coordinates: C1: $(-7.55, 25.3)$, C2: $(-6.24, 33.2)$, C3: $(-5.31, 42.1)$ C4: $(5.55, 25.3)$, C5: $(6.34, 33.2)$, C6: $(7.14, 42.1)$
Ground Wire Coordinates	G1: $(-8.54, 50.3)$, G2: $(8.54, 50.3)$
Tower Span	400 m
Tower Footing Resistance	5–20 Ω
Line Reactor Rating	63 MVAr at 400 kV (per circuit at Adani end)

TABLE F.2: Equivalent Source Impedance Data

Impedance Parameter	Adani (Ω)	Rahanpur (Ω)
R_1 (Positive-sequence resistance)	0.12	1.49
X_1 (Positive-sequence reactance)	27.2	20.02
R_0 (Zero-sequence resistance)	2.02	1.49
X_0 (Zero-sequence reactance)	27.12	20.02

TABLE F.3: Surge Arrester (SA) Data

Parameter	Value
Rated Voltage, U_r (kV rms)	360
Maximum Continuous Operating Voltage, U_c (kV rms)	288
Rated Frequency	50 Hz
Nominal Discharge Current (8/20 µs)	10 kA
High Current Impulse (4/10 µs)	100 kA
Switching Surge Protective Level (500 A, 30/60 µs)	780 kV
Lightning Impulse Protective Level (10 kA, 8/20 µs)	960 kV
Steep Current Impulse Protective Level (3 kA, 1/2 µs)	1010 kV
Reference Voltage V_{ref} (1 mA DC)	280 kV
Residual Voltage at 5 kA (8/20 µs)	900 kV
Residual Voltage at 10 kA (8/20 µs)	960 kV
Nonlinear Coefficient α	25
Energy Absorption Capability (4/10 µs)	12 kJ/kV of U_r
Creepage Distance	$\geq$ 8500 mm
Insulation Type	Composite Polymer / Porcelain

Appendix G
Circuit Model and Observed Waveforms for Switching Transient Overvoltage Case Study

The switching transient study is carried out on the Adani–Rahanpur 400 kV double-circuit transmission line as a case study. The circuit model developed in PSCAD for this purpose is shown in Fig. G.1. The parameters of the frequency-dependent phase model used to represent the Adani–Rahanpur 400 kV double-circuit line are illustrated in Fig. G.2.

The observed voltage waveforms from line energization and line re-energization studies for Circuit 1 of the Adani-Rahanpur transmission line—under different control strategies (no control, PIR control, and SA control)—are presented in Fig. G.3 and Fig. G.4, respectively.

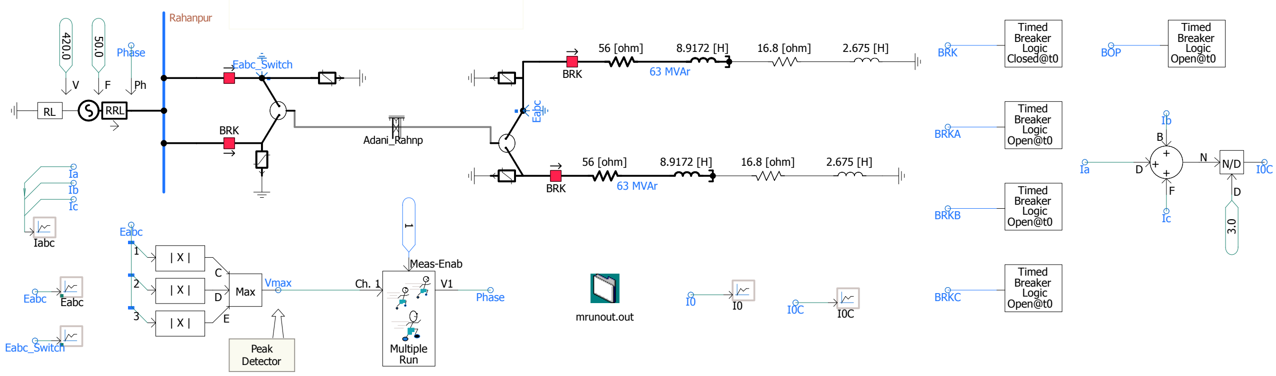

Fig. G.1: Circuit model developed in PSCAD for switching transient overvoltage case study

Definition Canvas (Adani_Rahnp)

Segment Name: Adani_Rahnp

Steady State Frequency: 50.0 [Hz]

Length of Line: 133.7 [km]

Number of Conductors: 6

Frequency Dependent (Phase) Model Options

Travel Time Interpolation: On
Curve Fitting Starting Frequency: 0.5 [Hz]
Curve Fitting End Frequency: 1.0E6 [Hz]
Total Number of Frequency Increments: 100
Maximum Order of Fitting for Yc: 20
Maximum Fitting Error for Yc: 0.2 [%]
Max. Order per Delay Grp. for Prop. Func.: 20
Maximum Fitting Error for Prop. Func.: 0.2 [%]
DC Correction: Disabled
Passivity Checking: Disabled

Tower: 3H5
Conductors: chukar
Tower Centre 0 [m]
Ground_Wires: ACSRDorking

Circuit #	Cond. #	Connection Phasing #	X (from tower centre)	Y (at tower)
	1	1	-7.55 [m]	25.3 [m]
	2	2	-8.34 [m]	33.45 [m]
	3	3	-7.14 [m]	42.1 [m]
	4	4	7.55 [m]	25.3 [m]
	5	5	8.34 [m]	33.45 [m]
	6	6	7.14 [m]	42.1 [m]

GW. #	Connection Phasing #	X (from tower centre)	Y (at tower)
1	Eliminated	8.54 [m]	50.3 [m]
2	Eliminated	-8.54 [m]	50.3 [m]

.4572 [m]

Resistivity: 100.0 [ohm*m]
Aerial: Analytical Approximation (Deri-Semlyen)
Underground: Direct Numerical Integration
Mutual: Analytical Approximation (LUCCA)

Fig. G.2: Parameters of the frequency dependent phase model for the Adani-Rahanpur 400kV double circuit line

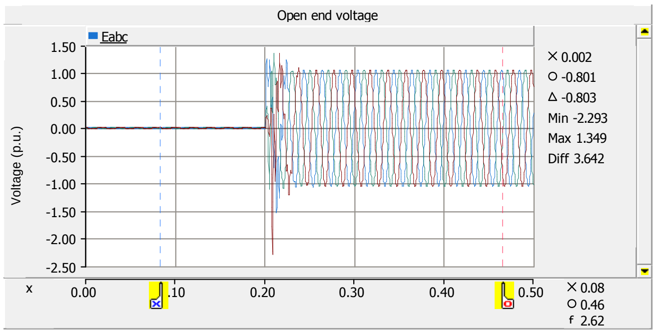

(a) Open end voltage (no control)

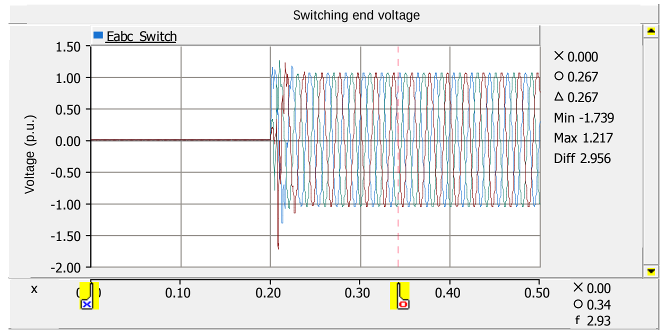

(b) Switching end voltage (no control)

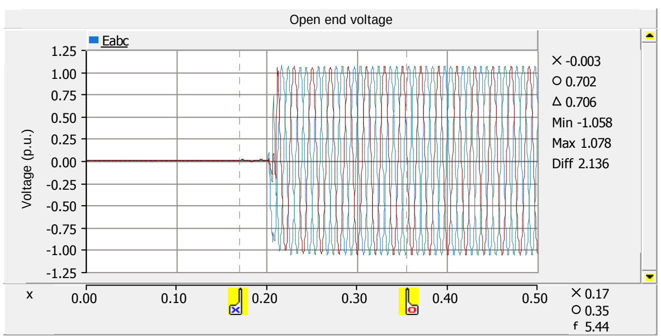

(c) Open end voltage (PIR 400 Ω, 8ms control)

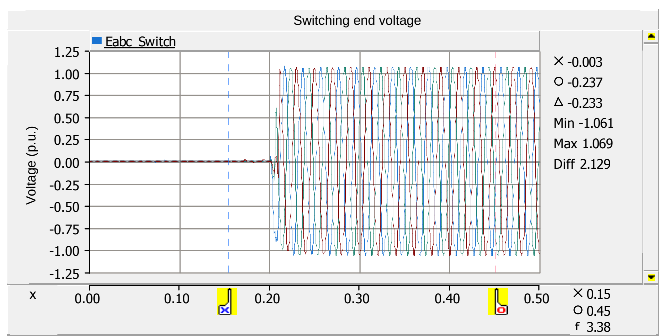

(d) Switching end voltage (PIR 400 Ω, 8ms control)

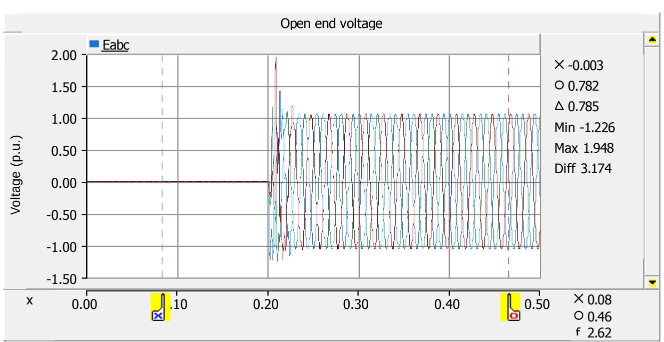

(e) Open end voltage (SA control)

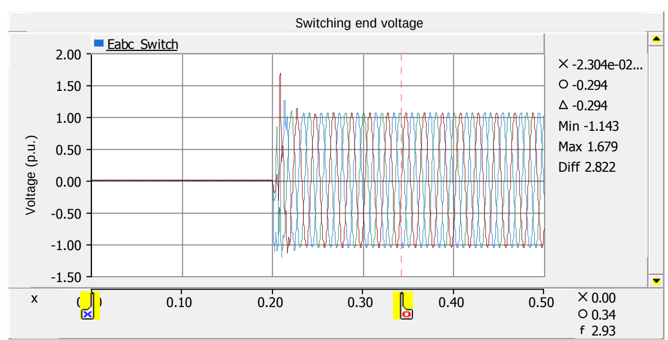

(f) Switching end voltage (SA control)

Fig. G.3: Voltage waveforms observed in line energization case study for circuit-1

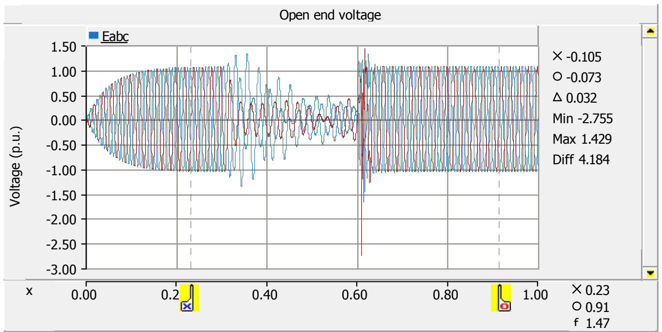

(a) Open end voltage (no control)

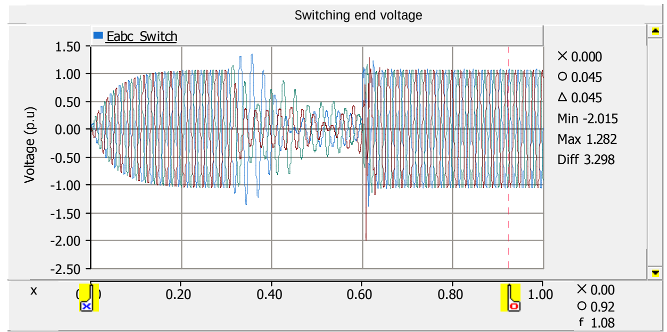

(b) Switching end voltage (no control)

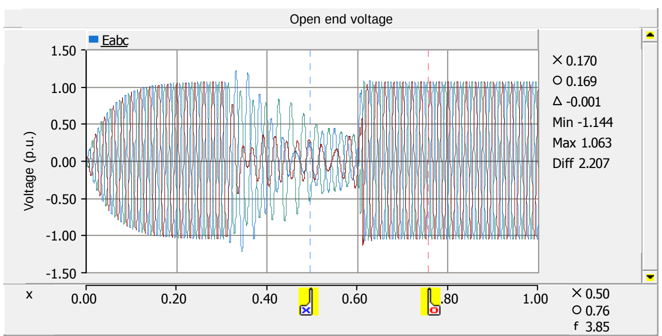

(c) Open end voltage (PIR-8ms control)

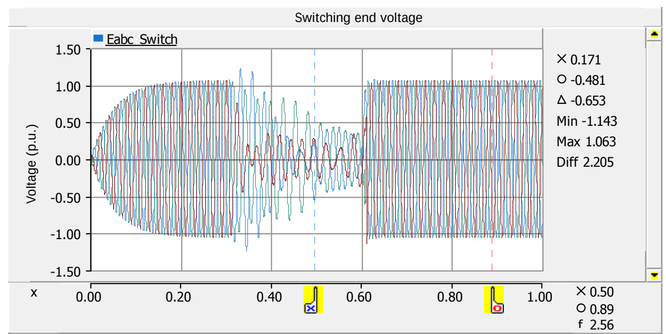

(d) Switching end voltage (PIR-8ms control)

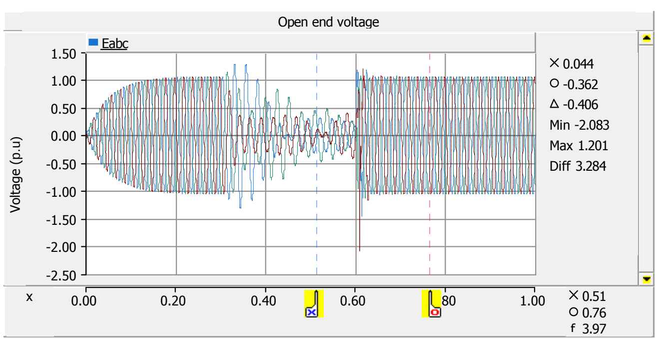

(e) Open end voltage (SA control)

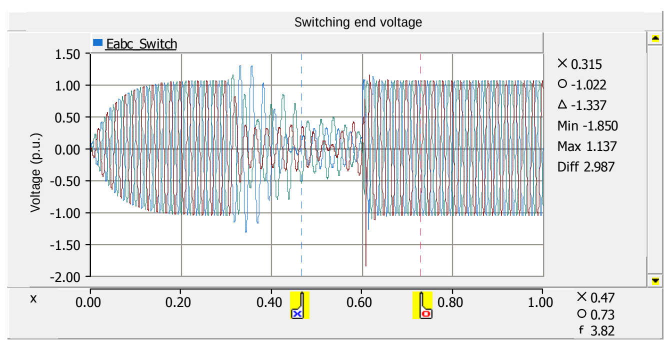

(f) Switching end voltage (SA control)

Fig. G.4: Voltage waveforms observed in line re-energization case study for circuit-1

Appendix H
Circuit Model and Observed Waveforms for NGR Design Case Study

The Adani–Rahanpur 400 kV double-circuit transmission line spans approximately 133.7 km, extending from the Adani Powerplant 400 kV switchyard in India to the Rahanpur 400 kV substation in Bangladesh. Each phase conductor is configured as a quad-bundled ACCC conductor, consisting of four sub-conductors. The line incorporates three transposition points. The first transposition is located approximately 44.5 km from either terminal. The second and third transpositions are positioned sequentially, each 22.25 km apart, following the first transposition point.

The steady-state analysis for NGR design in the Adani–Rahanpur 400 kV double-circuit shunt-compensated transmission line is conducted as follows:

a) Single Pole Switching: A SLG fault with single-pole switching is applied at three strategic locations along the line—namely, the sending end, midpoint, and receiving end. For each scenario, the NGR value is varied from 0% to 35% of the shunt reactor (X_s) in increments of 5%. The corresponding primary arc current, secondary arc current, and recovery voltage are recorded at the faulted location. For demonstration purposes, the PSCAD-developed circuit diagram and simulated waveforms for the case of an SLG fault at the line midpoint with an NGR value of 30% ($X_n/X_s = 30\%$) are shown in Fig. H.1, Fig. H.2, and Fig. H.3, respectively.

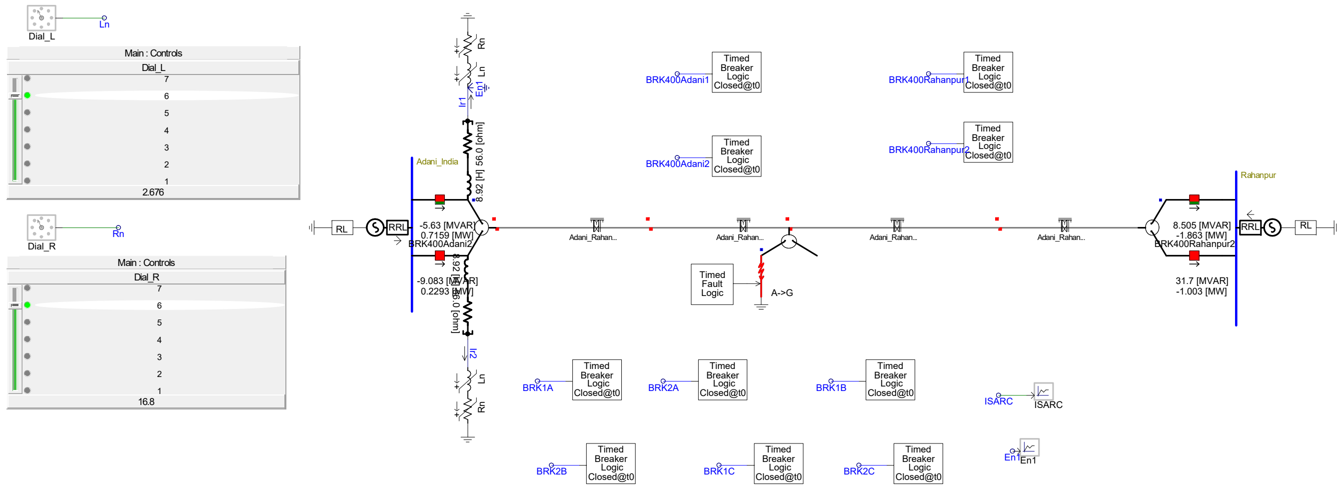

Fig. H.1: PSCAD circuit model for single-pole switching with midpoint SLG fault for NGR design

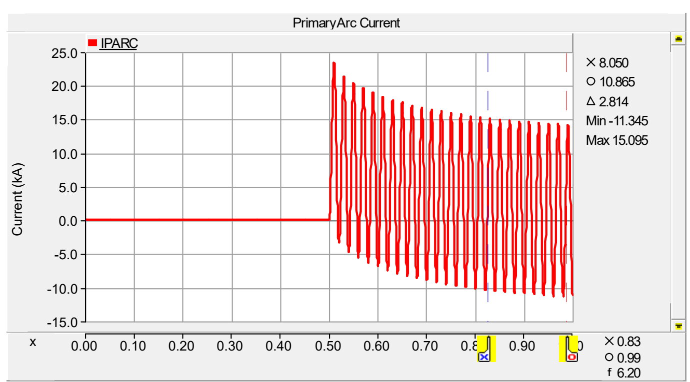

Fig. H.2: Primary arc current due to SLG fault applied at midpoint with X_n/X_s ratio of 30% (no single-pole switching is applied)

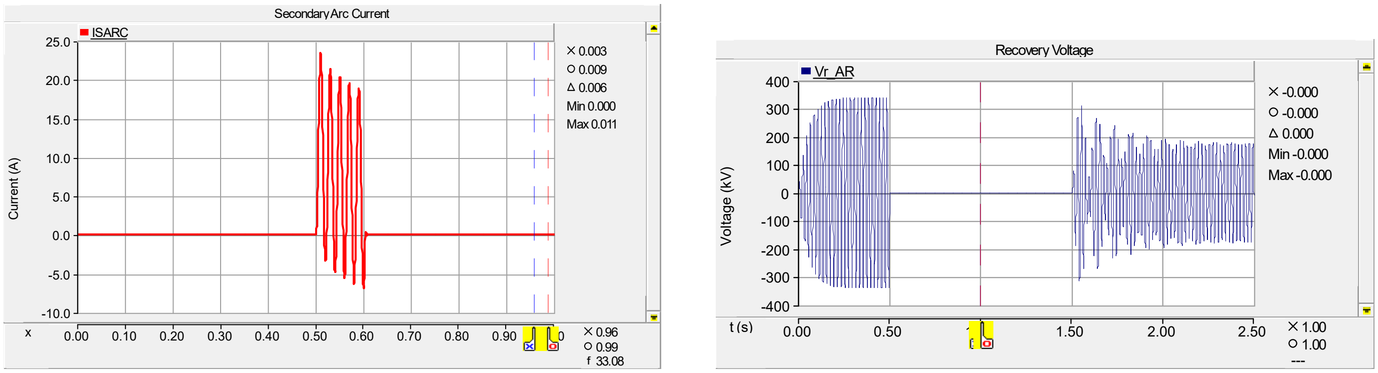

(a) Secondary arc current at fault location

(b) Recovery voltage at fault location

Fig. H.3: Secondary arc current and recovery voltage during single pole switching with SLG fault applied at midpoint for $X_n/X_s = 30\%$

b) Stuck Breaker Analysis: Eight stuck breaker conditions (presented in Appendix D) are simulated for the Adani–Rahanpur 400 kV double-circuit transmission line. For each condition, the NGR value varies from 0% to 35% of the shunt reactor in increments of 5%. For demonstration purposes, the developed PSCAD circuit model and the corresponding neutral voltage and current waveforms for two representative cases (Case 1 and Case 3) with an X_n/X_s ratio of 10% are presented in Fig. H.4, Fig. H.5, and Fig. H.6, respectively.

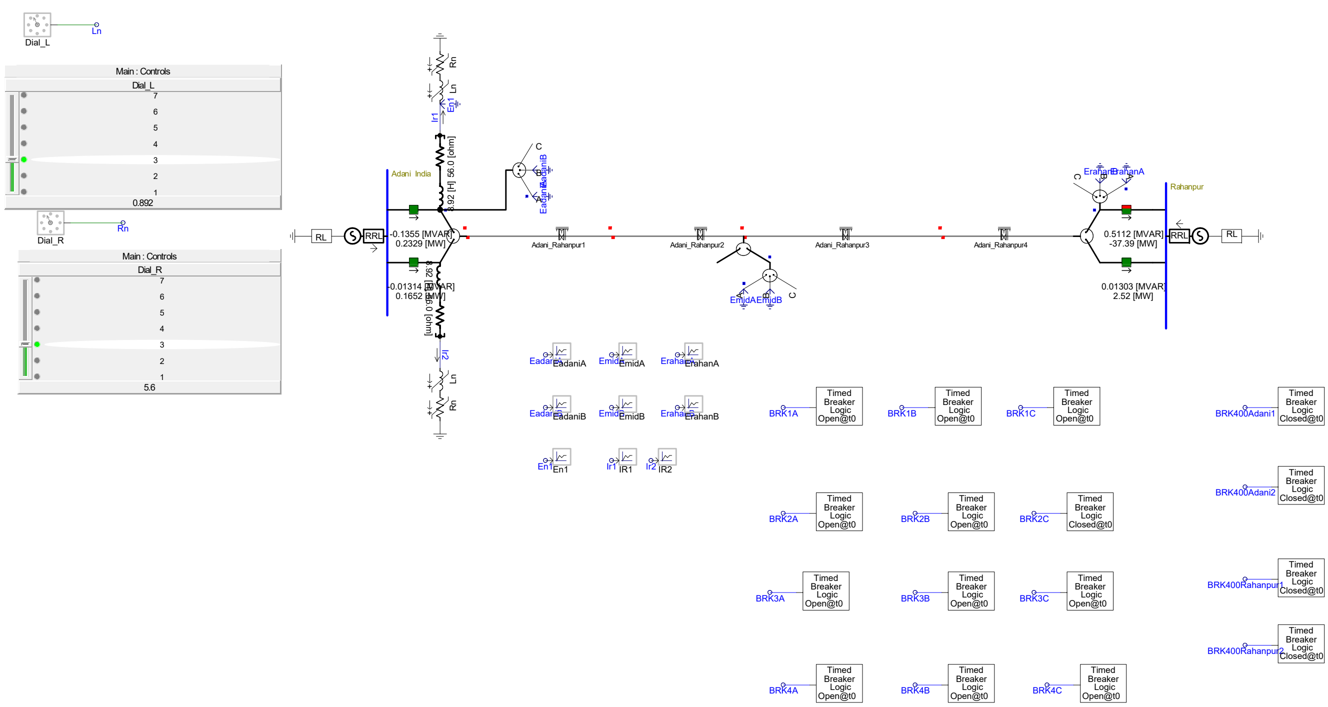

Fig. H.4: PSCAD circuit model for various stuck breaker conditions analysis for NGR design

c) Induced Voltages on De-energized Circuit: Since the Adani–Rahanpur 400 kV transmission line is a double-circuit configuration, this study evaluates the induced voltages on a de-energized circuit under two conditions: (i) energization of the adjacent circuit, and (ii) energization of the adjacent circuit followed by a SLG fault at various locations (Adani end, midpoint, and Rahanpur end). For both cases, the NGR value varies from 0% to 35% of the shunt reactor in increments of 5%. For illustration purposes, the PSCAD circuit model and the resulting maximum induced phase-to-ground and neutral voltages on the de-energized circuit—under the scenario where the adjacent circuit is energized with an SLG fault at the Adani end and $X_n/X_s = 5\%$—are shown in Fig. H.7 and Fig. H.8, respectively.

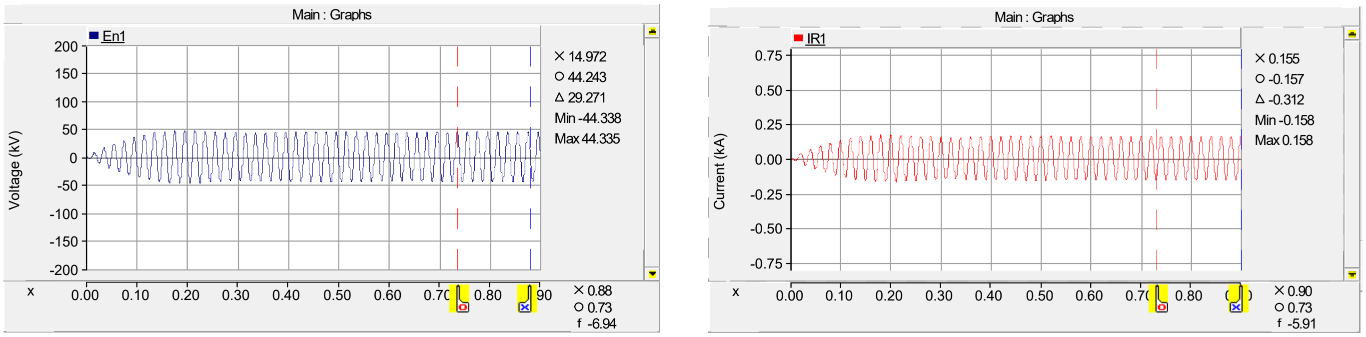

(a) Neutral voltage

(b) Neutral current

Fig. H.5: Neutral voltage and current during stuck breaker case-1 (single pole stuck breaker condition with remote end fully open and parallel line de-energized) for $X_n/X_s = 10\%$

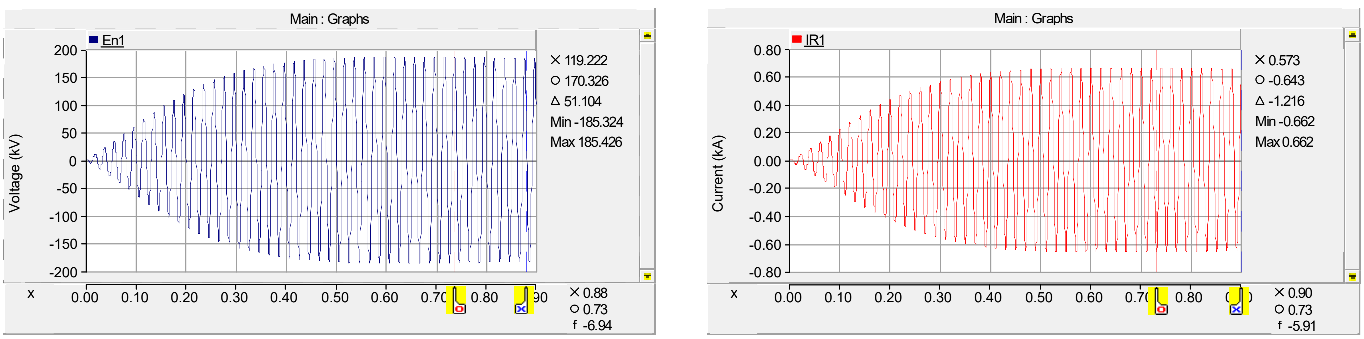

(a) Neutral voltage

(b) Neutral current

Fig. H.6: Neutral voltage and current during stuck breaker case-3 (two pole stuck breaker condition with remote end fully open and parallel line de-energized) for $X_n/X_s = 10\%$

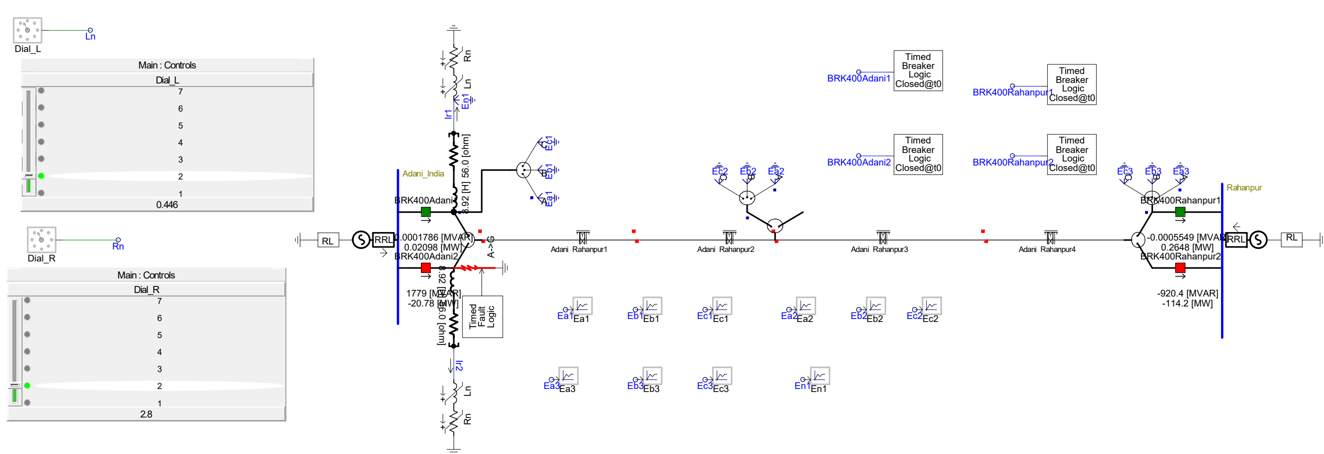

Fig. H.7: PSCAD circuit model for induced voltage study on de-energized circuit for NGR design

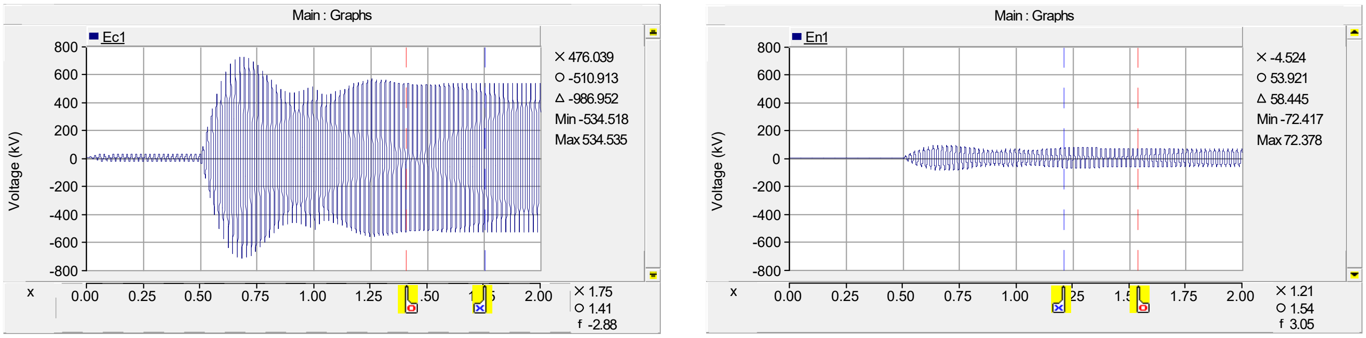

(a) Phase-to-ground voltage

(b) Neutral voltage

Fig. H.8: Induced phase-to-ground and neutral voltage on de-energized circuit by energizing the adjacent circuit with SLG fault at Adani end for X_n/X_s = 5%

The transient studies—including line energization and single-pole auto-reclosing (open and reclose)—validate the preliminary NGR rating determined from steady-state analyses. These dynamic studies assess whether the selected NGR effectively mitigates overvoltages, limits secondary arc currents, and satisfies the required breaker dead time for successful auto-reclosure.

d) Single-Pole Auto-Reclosing: The single-pole auto-reclosing study considers SLG faults applied at three locations along the Adani–Rahanpur 400 kV transmission line: the Adani end, midpoint, and Rahanpur end. The analysis is carried out using the selected NGR value of $840\,\Omega$. For illustration purposes, the PSCAD-developed circuit model and the observed recovery voltage and secondary arc current at the fault location—corresponding to an SLG fault at the Rahanpur end—are presented in Fig. H.9 and Fig. H.10, respectively.

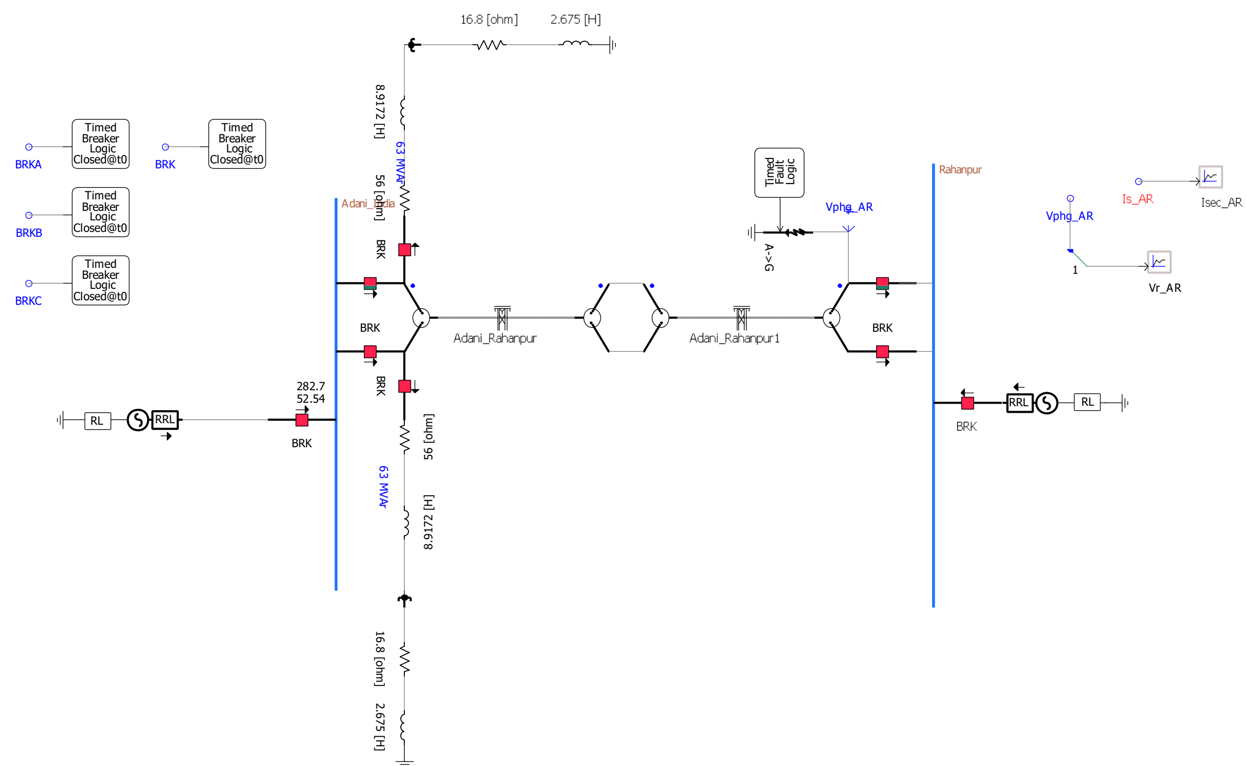

Fig. H.9: PSCAD circuit model for single-pole auto-reclosing study (SLG fault applied at Rahanpur end) for NGR design

e) Switching Overvoltage Study: Line energization is simulated for the Adani–Rahanpur 400 kV transmission line using the selected NGR value of $840\,\Omega$ in the presence of SA protection. Switching overvoltages are monitored

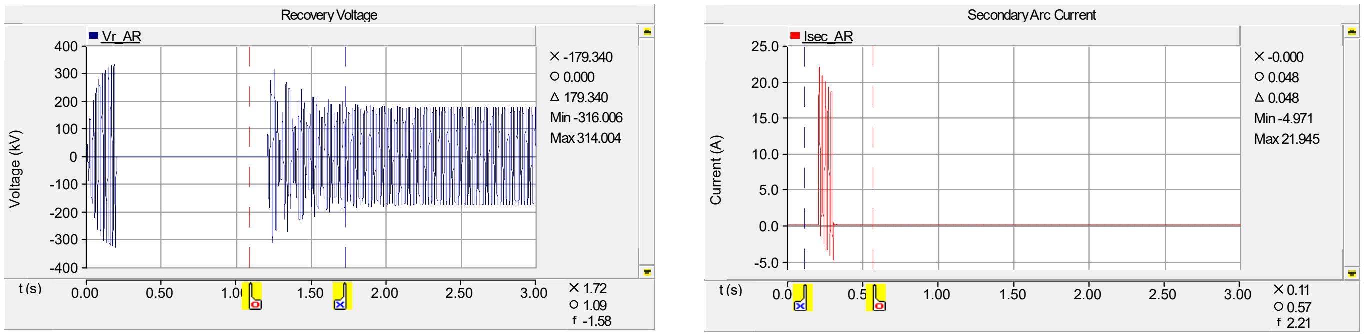

(a) Recovery voltage at fault location

(b) Secondary arc current at fault location

Fig. H.10: Recovery voltage and secondary arc current during single-pole auto-reclosing study by applying SLG fault at Rahanpur end with the selected NGR value of 840Ω

at the switching end, midpoint, and open end of the line. For illustration purposes, the PSCAD-developed circuit model and the corresponding switching overvoltage waveforms—obtained during energization by closing the circuit breaker at the Rahanpur end—for circuit-1 are presented in Fig. H.11 and Fig. H.12, respectively.

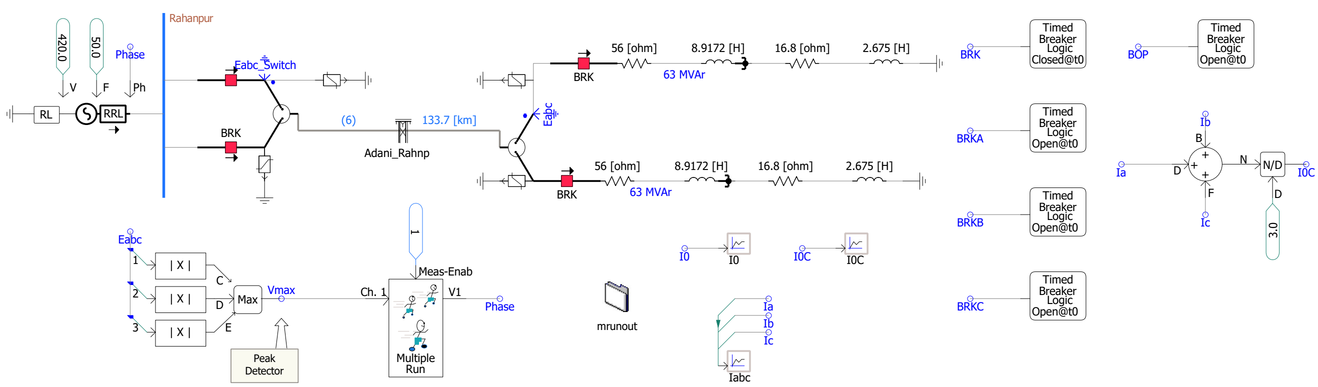

Fig. H.11: PSCAD circuit model for switching transient study for NGR design

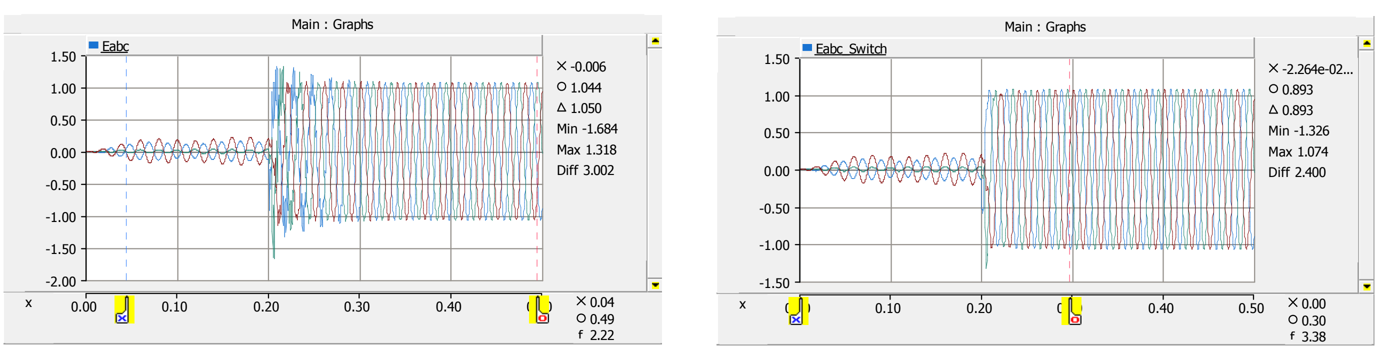

(a) Adani end (open end)

(b) Rahanpur end (switching end)

Fig. H.12: Switching transient overvoltages observed in circuit-1 due to line energization with the selected NGR value of 840Ω and with SA protection

APPENDIX I
RECOMMENDED NGR PARAMETERS FOR ADANI-RAHANPUR 400KV DOUBLE CIRCUIT TRANSMISSION LINE

The recommended specifications of the NGR, along with the corresponding selection basis for the Adani–Rahanpur 400 kV double-circuit shunt-compensated transmission line, are provided in Table I.1.

TABLE I.1: Recommended NGR parameters for Adani-Rahanpur 400 kV double circuit transmission line

Parameter	**Recommended Value**	**Selection Basis**
Rated Impedance	$840\,\Omega$	From steady-state analysis, steady-state secondary arc current and RRRV are observed to be less than $40\,\mathrm{A_{rms}}$ and $10\,\mathrm{kV/ms}$ respectively. No substantial resonance overvoltages are observed with the proposed NGR value of $840\,\Omega$ (30% of X_s). From transient studies, a dead time of 1 s is satisfied for single-pole auto-reclosing and switching overvoltages remain within the BSIL limits of the transmission system.
Short-time (10 sec) Thermal Current and Voltage Rating	$100\,\mathrm{A_{rms}}$, $70\,\mathrm{kV_{rms}}$	From steady-state analysis, the observed maximum temporary neutral voltage and current are $68\,\mathrm{kV_{rms}}$ and $70\,\mathrm{A_{rms}}$, respectively. Hence, the thermal rating is selected as $70\,\mathrm{kV_{rms}}$, $100\,\mathrm{A_{rms}}$.
Continuous Current and Voltage	$5\,\mathrm{A_{rms}}$, $4.2\,\mathrm{kV_{rms}}$	As per IEEE Std C57.32-2015 [13], 3% of the thermal current rating is $3\,\mathrm{A_{rms}}$. Considering a safety factor, the continuous current rating is proposed as $5\,\mathrm{A_{rms}}$. The corresponding voltage at $840\,\Omega$ is $4.2\,\mathrm{kV_{rms}}$.
Rated Peak Current	$370\,\mathrm{A_{peak}}$	Based on transient studies, the maximum initial asymmetric peak current flowing through the neutral is observed to be approximately 303 A at the selected NGR value. From IEEE Std C57.32-2015 [13], the rated peak current is calculated as $I_{\text{peak}} = K \cdot I_{\text{rms}}$, where $K = 3.3$ and $I_{\text{rms}} = 100\,\mathrm{A}$. Hence, $I_{\text{peak}} = 3.3 \cdot 100 = 330\,\mathrm{A}$. Based on these findings and considering 10% safety factor, a rated peak current of 370 A is proposed. The multiplier $K = 3.3$ is derived from IEEE Std C57.32-2015 [13], which suggests using the expression $K = 1.2(1 + e^{-\pi R/X})$. The study system has an X/R ratio of 50.
Voltage Class and Insulation Level at Neutral Point	$69\,\mathrm{kV_{rms}}$, BIL = $350\,\mathrm{kV_{peak}}$	Based on steady-state and transient studies, the observed maximum temporary neutral voltage is $68\,\mathrm{kV_{rms}}$. As per IEEE Std C57.32-2015 [13], a $69\,\mathrm{kV_{rms}}$ insulation class and $350\,\mathrm{kV_{peak}}$ BIL are proposed.
Surge Arrester Rating for NGR	$66\,\mathrm{kV_{rms}}$ rated; $74.2\,\mathrm{kV_{rms}}$ TOV	Rated voltage of $66\,\mathrm{kV_{rms}}$; 10-second TOV withstand capability of $74.2\,\mathrm{kV_{rms}}$. Proposed based on temporary overvoltage requirement of $70\,\mathrm{kV_{rms}}$ for 10 seconds.

APPENDIX J
PROJECT SIMULATION FILES REPOSITORY

The project related PSCAD simulation files can be accessed from the following Github repository. Link: https://github.com/MdTouhidulHaque/ECE633_Project